ARTICLES

Gas-Phase Reactivity of Selected Transition Metal Cations with CO and CO_2 and the Formation of Metal Dications Using a Sputter Ion Source

Jamie Herman, Jeremy D. Foutch, and Gustavo E. Davico*

Department of Chemistry, University of Idaho, P.O. Box 442343, Moscow, Idaho 83844

Received: November 22, 2006; In Final Form: January 29, 2007

Reaction products and rates were measured for the gas-phase reactions of selected first row transition metal ions (Ti^+, V^+, Fe^+, Co^+, Ni^+, Cu^+, Zn^+) and both CO and CO_2 using a flowing afterglow instrument. The formation and description of products formed and reaction mechanisms are presented and discussed as well. Ab initio calculations were used to produce potential-energy surface diagrams for selected reactions as a tool to further understand the reaction mechanisms, thermochemistry, and reaction kinetics. Reactions with CO are slow and typically yield complexes of the form $M(CO)_n^+$ ($n = 1-2$), with the second CO molecule appearing to be added faster than the first one. Reactions with CO_2 also yield the formation of clusters; however, in the case of Ti^+, the reaction produces the oxide TiO^+ ion efficiently. An interesting observation was also the formation of metal doubly charged ions. Some dications were easily obtained as the major ion by changing the ionization conditions in the sputter ion source. We are proposing an ionization mechanism for the formation of the dications.

Introduction

Transition-metal cations and many of their compounds are important species that display very different chemical properties. Their rich and highly diverse chemistry is mostly due to the partially filled near degeneracy of the s and d orbitals that could result in the low-lying energy excited states being populated even at room temperature. The benefits of understanding the chemistry of these reactions, however, have extended beyond the realm of chemists alone and have now become a topic of interest to multiple disciplines of science. However producing metal cations in the gas phase has its limitations, and special instrumentation and techniques have been developed to overcome this challenge. Some of these methods to promote metal cations into the gas phase involve quite energetic processes. To obtain an accurate characterization of the reactions of these metal cations, the excess energy must be sufficiently relieved prior to reaction, as in the flowing afterglow instrument.[1] Insufficient thermalization may result in inflated rate data for favorable reactions and/or the formation of reaction products that would not otherwise be energetically favored.

Efforts to develop better methods for CO_2 sequestration have become particularly important with increased awareness of the accumulation of greenhouse gases from a variety of anthropogenic emission sources. Carbon dioxide is the fifth most abundant atmospheric gas and the most abundant gas known to contribute to the greenhouse effect. Therefore, it is technologically and environmentally important to be able to sequester carbon dioxide emissions and/or to transform this gas into more benign and useful compounds. However, CO_2 is thermodynamically very stable and consequently not very reactive; therefore, it needs to be activated before utilization. Transition metal cations and their compounds are good candidates to catalyze this reaction and may prove useful in the effort to help control CO_2 emissions.

Transition-metal cations and many compounds incorporating metal cations also display the ability to catalyze a variety of organic and biological reactions. In some proteins carbon monoxide, which often binds strongly to these metal centers, is required for the enzyme to show activity.[2] It is an interesting dichotomy that carbon monoxide is extremely toxic (because it binds to hemoglobin tighter than oxygen does and displaces oxygen) and yet may be needed for enzymatic activity. Therefore, the question as to why enzymes in living organisms require carbon monoxide in order to be active should be raised. It is possible that the requirement for CO could be an evolutionary relic—one that is still necessary for function but that indicates the molecular diversity present either in the primordial broth from which life evolved or in the largest and most diverse chemical lab: the interstellar space. Although some transition metal−carbonyl complexes are known in the condensed phase, experimental data about these reactions in the gas phase is not abundant and data is sometimes contradictory. The Fe^+−CO system is very interesting since there is some evidence suggesting that the product ion might have been observed in interstellar dust.[3] We also hope that these laboratory results would encourage astronomers to look at spectroscopic signatures of metal carbonyl complexes in interstellar space.

In this article we are reporting experimental results on the reactions of Ti^+, V^+, Fe^+, Co^+, Ni^+, Cu^+, and Zn^+ with CO and CO_2. A few of the reactions rates with CO have been reported in the literature; however, data is scattered, obtained

* To whom correspondence should be addressed. E-mail: davico@uidaho.edu.

10.1021/jp067777k CCC: $37.00
Published on Web 03/09/2007

under different conditions making comparisons difficult, and occasionally only upper bound figures are reported.[4−6] Rate constants for the reactions with CO_2 were reported while this article was been written; however, only lower bound values were reported again for most reactions.[7] Some of the data is contradictory. For instance, the reaction rate for Fe^+ was reported as $<10^{-15}$ and $\geq 5 \times 10^{-13}$ cm^3 molecule^{-1} s^{-1} by the same research group using similar instrumentation.[7,8] Also similar conflicting results were reported for the reaction of V^+.[7,9,10] Therefore, a systematic study of these reactions is warranted. Density functional theory (DFT) results for some of these reactions are also reported in this article as a tool to further understand product formation and reaction mechanisms as well as reactivity. In addition, the synthesis of multiply charged cations for these transition metals is also discussed and a mechanism for producing these species and their argon clusters is proposed.

Experimental Section

A flowing afterglow instrument was used to study these reactions and to determine their reaction rates. This system has been previously described in great detail,[1,11] including specific details about our instrument.[12] Special modification to our instrument for this work includes a sputter ion source for the generation of metal ions. The design of the sputter ion source is similar to the one described by Lineberger for the production of negative ions,[13,14] and it is inserted upstream and on the side of the flowing afterglow tube. A relatively small amount of argon is mixed with the helium buffer gas to promote sputtering. Typical experimental conditions involve 13 SLM of helium, and the argon flow is adjusted between 0.06 and 0.7 SLM (0.5−5%) to optimize the target ion signal. Although a mass flow controller is located on the helium line only, argon flow was determined simply by noting the change in the flow tube pressure before and after the argon valve was opened and then increasing helium flow in the absence of argon until that same flow tube pressure was once again reached. The observed change in helium flow was then recorded as the argon flow, and the total gas flow (argon plus helium) was used to determine the rate constants. Gas purities were: helium (99.95%), argon (99.95%), CO (99.0), and CO_2 (99.99%). Helium flows were directed through a liquid-nitrogen-cooled, high-efficiency molecular sieve trap, and other gases were used without further purification. For these metals only monatomic cations are observed under these conditions.

The focus of this study involved several of the first-row transition metals, including Zn^+, Cu^+, Ni^+, Co^+, Fe^+, V^+ and Ti^+. Purities of the metals were: Ti (99.99%), V (99.8%), Fe (99.9+%), Co (99.9+%), Ni (99.9+%), Zn (99.99%), and Cu (99.99%). Each metal was individually sputtered, introducing cations into the reaction flow tube. CO and CO_2 gases were then added in separate trials through one of the seven inlets along the flow tube, mass spectra were collected, and products identified. Fast rate constants ($\geq 10^{-11}$ cm^3 molecule^{-1} s^{-1}) were determined by following the disappearance of the reactant ion. This determination is automated and typical results were published before.[12] Slower rate constants were determined by following the appearance of the detectable product ions. In these cases a large flow of neutral gas (CO or CO_2) is required, which usually changes the flow characteristics and the ion diffusion producing an increase in the reactant ion signal at longer reaction times. This behavior has been observed before on a similar instrument.[5,7] It is possible to use only the reactant ion data from the first few inlets to extract the rate constants; however, we used eqs 1−4 instead to calculate the pseudo-first-order rates following the formation of the ionic products.[15] Formation of higher-order products can also be determined by using eq 3 or 4 in selected cases. Thus, we evaluated the appropriate expression at each inlet (e.g., time) and used a nonlinear least-squares fitting to obtain values for k_1 and k_2

$$M^+ \xrightarrow[k_1]{N} P_1 \xrightarrow[k_2]{N} P_2 \tag{1}$$

$$1 - \frac{[P_1]}{[M^+]} = e^{-k_1 t} \tag{2}$$

$$\frac{[P_1]}{[M^+]} = y_0 + \frac{k_1}{k_2 - k_1}(e^{-k_1 t} - e^{-k_2 t}) \tag{3}$$

$$1 - \frac{[P_2]}{[M^+]} = \frac{k_2}{k_2 - k_1} e^{-k_1 t} - \frac{k_1}{k_2 - k_1} e^{-k_2 t} \tag{4}$$

First-order ionic product rates were thus determined by a nonlinear least-squares fit using eq 2 if no secondary reaction was observed. When secondary reactions were detected the product ion signal was usually fitted using eq 3; however, eq 4 was also used to confirm the results if enough P_2 ion signal was available.

It should be remembered that most of these reactions are actually termolecular in nature, with helium providing collisional stability to the formation of metal−ligand clusters and any subsequent association product. We ran test rate constant measurements for some of the reactions studied at varying helium flows. Helium flows (hence pressures) were increased to 16−18 SLM; however, no statistical difference was observed in the measured rates of product formation with respect to those obtained at 13 SLM helium flow. Rate constants were measured at least three times at 298 ± 2 K, and the reported errors are one standard deviation of the final rate constant values or one standard deviation of the fitting procedure, whichever is larger.

All calculations were performed with the Gaussian 98 suite of programs.[16] Geometry optimizations and frequency calculations as well as zero-point energies (ZPE) were carried out using density functional theory (DFT). The B3LYP hybrid exchange-functional[17−19] was used with the 6-31+G(d) and aug-cc-pVDZ basis sets for the metal monocations and carbon and oxygen atoms, respectively.[20,21] The B3LYP/6-311G(d) model was used for the metal dication−argon clusters for both metal and argon atoms. The geometry of each stationary point was completely optimized at the appropriate level of theory within the molecular symmetry. The stability of the wave function was checked and re-optimized until no further substitutions afforded lower energies, as several low-lying excited electronic states are observed in structures involving transition metals. The number of negative eigenvalues in the Hessian was used to determine if a structure is a minimum, transition state, or higher order saddle point. IRC calculations were performed for all the transition states to ensure that they connect the reported minima.

Results and Discussion

Reactions of Monocations with CO. The results obtained for these reactions are listed in Table 1 showing that complexation is the only observed product and indicating that the reaction rates of the metal cations being studied with CO are quite slow insomuch that rate constants for complex formation were obtainable for only Zn^+, Cu^+, Ni^+, and V^+. In general these results are consistent with other experimental results

TABLE 1: Products and Observed Rate Constants for the $M^+ + CO$ Reactions

reaction	product	k_{obs}[a]	k_{lit}[a]	efficiency[b]	higher-order products
$Ti^+ + CO$	NR[c]	NR		0	
$V^+ + CO$	$V(CO)^+$	0.7 ± 0.2		9×10^{-5}	
$Fe^+ + CO$	NA[d]	NA	<0.1,[e] <2[f]	0	
$Co^+ + CO$	$Co(CO)^+$	NA[g]			
$Ni^+ + CO$	$Ni(CO)^+$	1.2 ± 0.3	5.6[h]	1.4×10^{-4}	$Ni(CO)_2^+$
$Cu^+ + CO$	$Cu(CO)^+$	7.8 ± 1.4	2.8[h]	1.0×10^{-3}	$Cu(CO)_2^+$
$Zn^+ + CO$	$Zn(CO)^+$	≤ 1		$\leq 1 \times 10^{-4}$	

[a] Observed rate constant in units of 10^{-13} cm^3 molecule^{-1} s^{-1}. [b] Reaction efficiency, k_{obs}/k_{col}, where the collision rate (k_{col}) is calculated according to reference 24. [c] NR: no reaction observed. [d] NA: not available due to superposition of peaks, see text for details. [e] From ref 6. [f] From ref 4. [g] NA: not available. Data too scattered for a reliable fit, see text for details. [h] From ref 5.

reported in the literature.[4,5,22] In some of the fastest reactions sequential termolecular addition of CO was also observed. The transfer of an oxygen atom, carbon atom, or an electron from CO to any of these metals is highly endothermic and therefore unfavorable and not observed.[23]

There are no reaction rates reported in Table 1 for Ti^+, Fe^+, and Co^+. There is no observable product in the reaction of Ti^+ with CO, and $Ti^+(CO)$ was not detected above the noise level even at very high CO flows, suggesting that the reaction rate for complexation is below our detection limit ($<1 \times 10^{-14}$ cm^3 molecule^{-1} s^{-1}). In the reaction of Co^+, the $Co^+(CO)$ complex is detected but kinetic results yield data too scattered for a reliable fit, suggesting a relatively slow reaction rate close to our detection limit. Our results also suggest a slow reaction rate for Fe^+. In this case, superposition of the $(CO)_2^+$ and $(CO)_3^+$ cluster ions peaks, present in small amounts in the flow tube, over the $^{56}Fe^+$ and $^{56}Fe^+(CO)$ peaks, respectively, prevents any definite answer. The superposition of these peaks can be avoided by following the less abundant $^{54}Fe^+$ (about 6% abundance) isotope. However, spectra show no discernible peak corresponding to $^{54}Fe^+(CO)$, which could be due to a slow rate constant or low isotope abundance and most probably to a combination of both.

The reaction of V^+ with CO produces a small but noticeable $V^+(CO)$ peak. The reaction rate is very slow and was measured to be 7×10^{-14} cm^3 molecule^{-1} s^{-1}. The reactions of Ni^+ and Cu^+ with CO are slightly faster and a higher-order complex, $M^+(CO)_2$, was also observed in these cases, in agreement with results from Jarvis et al.[25] Although the rates for the formation of the $M^+(CO)_2$ species could not be obtained, it seems that the addition of a second CO molecule is faster than the first, which is consistent with other sequential complexation reactions (see below) in which a larger (more degrees of freedom) complex would have a longer lifetime and therefore an increased chance to transfer excess energy to the helium buffer gas before dissociating back to reactants and thus reach the detector. Finally, only an upper limit value for the $Zn^+(CO)$ complex could be obtained for the reaction of Zn^+ with CO as the reaction rate is slow and data are too scattered for a reliable fit.

An upper limit for the rate constant for the reactions of Fe^+ with CO was reported in the literature. As seen in Table 1, Baranov et al.[6] reported it as $<10^{-14}$ cm^3 molecule^{-1} s^{-1}; however, the same authors reported later a higher upper limit of $<2 \times 10^{-13}$ cm^3 molecule^{-1} s^{-1}.[4] The absence of a peak corresponding to the $^{54}Fe^+(CO)$ species in our experiment is consistent with these results. Jarvis et al. reported the complexation kinetics of Ni^+ and Cu^+ with several ligands including CO using an instrument similar to ours;[5] their reported values for Ni^+ and Cu^+ are a little faster and slower than ours, respectively (Table 1). The source of the disagreement is uncertain at this time as our values are not consistently lower or higher than those reported in the literature. Thermalization

TABLE 2: Electronic States and Boltzmann Population Distributions for Transition Metal Cations Calculated at 298 K[a]

M^+	electronic configuration	term	J	population (%)	M^+	electronic configuration	term	J	population (%)
Ti	$[Ar]3d^24s$	a^4F	$^3/_2$	46.51		$[Ar]3d^7$	a^4F	$^9/_2$	0.01
			$^5/_2$	29.53				$^7/_2$	0.00
			$^7/_2$	15.64				$^5/_2$	0.00
			$^9/_2$	6.96				$^3/_2$	0.00
			total[b]	98.64				total[b]	0.01
	$[Ar]3d^3$	b^4F	$^3/_2$	0.58	Co	$[Ar]3d^8$	a^3F	4	98.95
			$^5/_2$	0.40				3	1.01
			$^7/_2$	0.24				2	0.04
			$^9/_2$	0.13				total[b]	100.00
			total[b]	1.36		$[Ar]3d^74s$	a^5F	5	0.00
	$[Ar]3d^24s$	a^2F	$^5/_2$	0.00				4	0.00
			$^7/_2$	0.00				3	0.00
			total[b]	0.00				2	0.00
V	$[Ar]3d^4$	a^5D	0	33.36				1	0.00
			1	28.03				total[b]	0.00
			2	19.94	Ni	$[Ar]3d^9$	^2D	$^5/_2$	99.93
			3	12.17				$^3/_2$	0.07
			4	6.49				total[b]	100.00
			total[b]	100.00	Cu	$[Ar]3d^{10}$	^1S	0	100.00
	$[Ar]3d^34s$	a^5F	1	0.00		(first excited-state at 21928.75 cm^{-1})			
			2	0.00	Zn	$[Ar]3d^{10}4s$	^2S	$^1/_2$	100.00
			3	0.00		(First excited-state at 48481.08 cm^{-1})			
			4	0.00					
			5	0.00					
			total[b]	0.00					
Fe	$[Ar]3d^64s$	a^6D	$^9/_2$	81.92					
			$^7/_2$	12.79					
			$^5/_2$	3.27					
			$^3/_2$	1.28					
			$^1/_2$	0.73					
			total[b]	99.99					

[a] Data taken from ref 27. Electronic states within 15 kcal mol^{-1} of the ground-state energy are included in the calculation. [b] Running total for all microstates within the specified electronic level.

TABLE 3: Products and Observed Rate Constants for the $M^+ + CO_2$ Reactions

					higher-order products	
reaction	product	k_{obs}[a]	k_{lit}[b]	eff[c]	product	k_{obs}[a]
$Ti^+ + CO_2$	$TO^+ + CO$	$(1.6 \pm 0.1) \times 10^{-10}$	4.1×10^{-11}	0.19	$TiO(CO_2)^+$	$\sim(2 \pm 1) \times 10^{-11}$
$V^+ + CO_2$	$V(CO_2)^+$	$(1.2 \pm 0.1) \times 10^{-12}$	$\geq 5 \times 10^{-13}$	0.002	$V(CO_2)_2^+$	$\sim(8 \pm 7) \times 10^{-12}$
$Fe^+ + CO_2$	$FeCO_2^+$	$(1.6 \pm 0.2) \times 10^{-12}$	$\geq 5 \times 10^{-13}$, $<10^{-15}$[d]	0.002	$Fe(CO_2)_2^+$	$\sim(3 \pm 2) \times 10^{-11}$
$Co^+ + CO_2$	$Co(CO_2)^+$	$(3.2 \pm 0.3) \times 10^{-12}$	$\geq 5 \times 10^{-13}$	0.004	$Co(CO_2)_2^+$	$\sim(3 \pm 2) \times 10^{-11}$
$Ni^+ + CO_2$	$NiCO_2^+$	$(8.2 \pm 2.0) \times 10^{-13}$	$\geq 5 \times 10^{-13}$	0.001	$Ni(CO_2)_2^+$	$\sim(2 \pm 1) \times 10^{-11}$
$Cu^+ + CO_2$	$CuCO_2^+$	$(2.9 \pm 0.2) \times 10^{-12}$	$\geq 4 \times 10^{-13}$	0.004	$Cu(CO_2)_2^+$	$(1.6 \pm 0.3)\ 10^{-11}$
$Zn^+ + CO_2$	$ZnCO_2^+$	$(3.4 \pm 0.9) \times 10^{-13}$	$\geq 7 \times 10^{-13}$	0.0004	NR[c]	

[a] Observed bimolecular rate constants in units of cm^3 $molecule^{-1}$ s^{-1}. [b] Literature values from ref 7 unless otherwise specified. [c] Reaction efficiency, k_{obs}/k_{col}, where the collision rate (k_{col}) is calculated according to reference 24. [c] NR: no reaction observed. [d] From ref 8

of the ions is an evident concern in the Jarvis report;[26] however, in the case of Cu^+, insufficient thermalization of the ion is not likely the cause of the disagreement since this ion is expected to be mainly in its ground electronic state as the term energy for the first excited electronic state is quite high, about 63 kcal/mol,[27] and would only be significantly populated at very high temperatures, as shown in Table 2. Thermalization of these atomic species is achieved by collisions with the helium buffer gas and argon from the sputter ion source or by radiative decay. The distance between the sputter ion source and the first neutral inlet in the reaction flow tube is about 50 cm in our instrument, larger than the usual 20−25 cm in this type of instrument, allowing for more collisions. In addition, the reaction flow tube pressure is maintained at about 0.5 Torr as opposed to 0.35 Torr in the ICP/SIFT apparatus.[4,25] Both of these factors ensure a better chance for thermalization of the ions before the reaction takes place. These factors could play a role in other ions as several low-lying excited states become readily available for metals located left of Cu in the periodic table in which *d* orbitals are partially filled, as it is shown in Table 2.

Results in Table 2 also show that insufficient thermalization becomes an increasing concern as moving from Cu to Ti in the periodic table. Although excited electronic states should be minimally populated if the ions are well thermalized, it is clear that even at room temperature Ti^+ shows substantial population in excited spin−orbit states. An indication that the ions are thermalized in our instrument is the absence of reaction between V^+ and CO_2 (vide infra). As suggested by one of the reviewers, another suitable test for ion thermalization is to introduce methane in our flow tube, as most ground-state metal cations will be unreactive with methane. We tried the reaction of Ti^+, the ion that is most likely to be in excited electronic state, with methane and we could not see any reaction at all to the limit of our detection suggesting once again that ions are thermalized in our system.

The trend in reactivity in these metals seems to follow the M−CO bond energy. Experimental dissociation energies for the M^+−CO complexes,[28−33] as well as comprehensive ab initio[34] and DFT[35] results for the complexation energy, show that the stability of the complexes increases with the metal atomic number for the metals included in this report, with the exception of Cu where a small decrease is predicted. Barnes et al. also concluded that the main component in the interaction between the metal centers and CO is electrostatic in nature and that promotion of electrons to unoccupied orbitals in the metal is also important to minimize repulsions with the CO molecule.[34] Although Zn was not included in these calculations, it can be speculated that its almost full s and d orbitals would increase the repulsions with the CO, decreasing the stability of the complex and therefore showing a slower association rate, which is consistent with the trend in rate constants shown in Table 1.

The M^+(CO) complexes show lower spin multiplicities than the atomic ion counterparts, most likely due to the electron redistribution that occurs upon complexation. The resulting surface crossing has been studied in detail by Glaesemann et al.[36] for the Fe system using correlated wavefunctions and could be responsible for the low reaction efficiency in these reactions as the M^+−CO bond is quite stable in relative terms. These authors show that the $^4\Sigma^-$ ground state of the Fe^+(CO) complex is bound by 29.7 or 22.7 kcal/mol with respect to the ^{6}D ground state of Fe^+ and CO depending on the theoretical level, CCSD-(T) or MCSCF, respectively. A larger experimental value for the Fe^+−CO D^0 of 36.6 ± 1.8 kcal/mol was also reported.[30] In addition, Barnes and co-workers reported M^+−CO bond energies ranging between 20 and 30 kcal/mol for the metals considered here at a lower theoretical level.[34] In any case, reaction efficiencies are small when considering the complexes' stability, suggesting that curve crossing might play a significant role during complexation.

Reactions with CO_2. The reactions of Ti^+, V^+, Fe^+, Co^+, Ni^+, and Cu^+ with CO_2 were also studied and the results are summarized in Table 3. A comprehensive article reporting the reactions of transition metal cations with CO_2 was published,[7] while this manuscript was being written. In general, these results agree with the values reported here, with the notable exception of Ti^+. Termolecular addition of CO_2 to the metals studied was observed generally to proceed at faster rates when compared with CO. The formation of $M(CO_2)^+$ clusters occurred for all metals with the exception of Ti^+, which strongly favored formation of the oxide, TiO^+, and it is the only truly bimolecular reaction included in Table 3. The double complex structures, $M(CO_2)_2^+$, were also observed to form with all metals except Zn^+ and Ti^+. In the latter case, subsequent formation of the $TiO(CO_2)^+$ cluster was also observed. In general, the formation of the double complex species was clearly observed to be faster than the rate of formation of the first complex despite the relatively larger errors in the rate constant values for the former.

Overall, data reported recently by Koyanagi et al.[7] agree with our observed bimolecular rate constants for the formation of the first CO_2 complex in the V^+−Zn^+ series, although these authors only report a lower limit value. In addition, these authors also observed higher-order complexes in agreement with results listed in Table 3. It is interesting to note that although Koyanagi et al. report a lower limit value of $\geq 5 \times 10^{-13}$ cm^3 $molecule^{-1}$ s^{-1} for the reaction of Fe^+,[7] the same authors reported an upper value of $<10^{-15}$ cm^3 $molecule^{-1}$ s^{-1} earlier using a similar instrument.[8] The source of the discrepancy is uncertain although Fe^+ ions were made using different ion sources in these reports.

The reactivity shown in Table 3 does not seem to follow the M^+−CO_2 bond dissociation energies (BDE). Sodupe and co-workers[10] published a comprehensive article reporting theoretical BDE for these metals ions (excluding Zn) with CO_2 at the B3LYP and CCSD(T) (ANO) levels and concluded that the interaction is mainly electrostatic in nature. Their BDE show a

minimum in Fe and a maximum in Ni, irrespective of the theoretical method used. Their results are in reasonable agreement with available experimental values for V^+,[9] Fe^+,[37−39] and Ni^+.[40] In contrast, the rate constants reported here for the formation of the CO_2 complexes show a monotonic increase from V^+ to Co^+, a decline in Ni^+, whereas Cu^+ is as fast as Co^+. The rate also decreases markedly for Zn^+. The discrepancy can be rationalized in terms of the required spin multiplicity change upon complexation and the fact that this crossing might not be very efficient and consequently the adiabatic well does not reflect in the reaction rates.

The dramatic change in reactivity of about 2 orders of magnitude between V^+ and Ti^+ warrants some further discussion. Koyanagi and co-workers[7] also observed the larger reaction rate in Ti^+; however, they reported a rate coefficient substantially slower than our value (see Table 3). The source of the discrepancy is not clear. These authors also report the rate for the reaction of Sc^+ to be slightly larger than that for Ti^+ but on the same order of magnitude. However, in the same article the Zr^+ and Hf^+ rates are also reported as $(2.5 \pm 30\%) \times 10^{-10}$ cm^3 $molecule^{-1}$ s^{-1} (with efficiencies of 0.34 and 0.37, respectively), indicating a large change in rates between the fourth and fifth periods (about 6 times faster) and negligible difference between the fifth and sixth periods of the periodic table in their data. In contrast, the reactivity of Ti^+ is only about 1.6 times faster than Zr^+ using our rate constant for Ti^+, which seems more reasonable in terms of the kinetic arguments discussed below. It can be argued that the Ti^+ reaction is slower due to a substantial barrier that can still be present in this reaction. If this is the case, the barrier should be much lower for the reaction of Sc^+; however, it is still slower than the reaction of Y^+ by a factor of 8.[7] Our larger value for Ti^+ could be attributed to insufficient ion thermalization in our instrument, which might be crucial in some of these ions (including Ti^+ and Zr^+); however, that seems unlikely as discussed above and considering that we recently measured the rate constants for Zr^+ and Nb^+ while studying the chemistry of their dications, and our values for these ions are in excellent agreement (within error bars)[41] with those reported by Koyanagi.[7]

The activation of the C−O bond in CO_2 by Ti^+ is very interesting. Sodupe and co-workers[10] reported high-level theoretical results of the thermochemistry of this activation (eq 5) for the first-row transition-metal ions (M = Sc−Cu). They concluded that the reaction is exothermic only for V^+, Ti^+, and Sc^+ and the driving force is the stronger M−O bond in these metals, which increases when going from Cu to Sc. Despite the reaction being exothermic for V^+, we do not detect C−O bond activation using this metal. This observation agrees with data reported recently;[7] however, it disagrees with earlier results reported by Sievers and Armentrout[9] which observed spontaneous formation of VO^+ using a guided ion beam experiments at CM kinetic energy close to 0 eV. The authors of the latter report acknowledge that the observed VO^+ ion could be the product of an insufficient thermalization of the parent ion or O_2 contamination

$$M^+ + CO_2 \rightarrow MO^+ + CO \qquad (5)$$

The reaction for M = V (eq 5) does not proceed despite being exothermic, suggesting a kinetic barrier which has been proposed to originate from an inefficient surface crossing between the quintet and triplet ground electronic states of reactants and products, respectively.[9,10] However, the reaction for M=Ti is relatively very efficient and exhibits an analogous surface crossing. To shed some light on the difference in reactivity of these ions we calculated the potential-energy surfaces (PES) for both ions at their higher and lower spin multiplicities. The results are plotted in Figures 1 and 2 for V^+ and Ti^+, respectively.

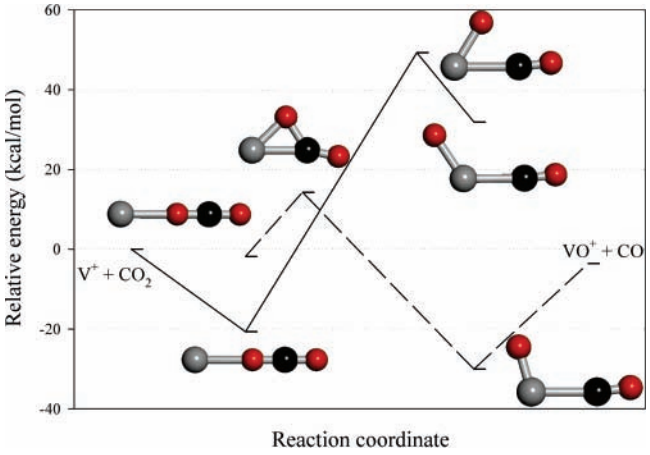

Figure 1. Schematic of the PESs calculated using DFT for the lowest quintet (solid line) and triplet (dashed line) electronic states for the reaction of V^+ with CO_2. Structures for some stationary points in the surface are also shown.

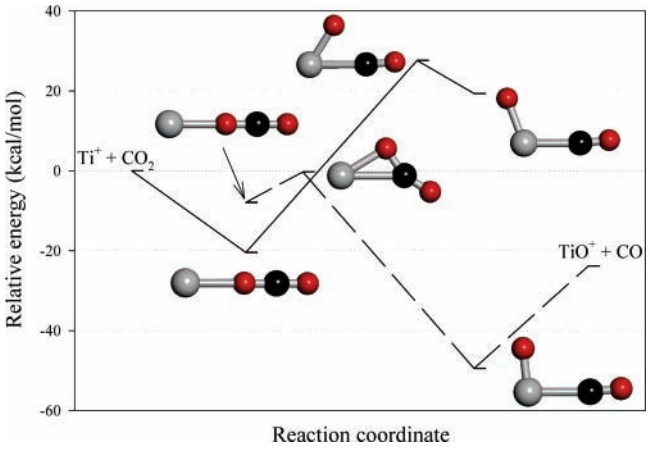

Figure 2. Schematic of the PESs calculated using DFT for the lowest quartet (solid line) and doublet (dashed line) electronic states for the reaction of Ti^+ with CO_2. Structures for some stationary points in the surface are also shown.

The schematic of the PES for V^+ (Figure 1) is similar to the one proposed earlier based on experimental thermochemical data on the reaction and product side complexes,[9] although with important differences. The most important difference is the position of the transition state for the reverse reaction, which in Figure 1 is located above the reactants suggesting that the curve crossing might occur above that level, therefore causing a substantial kinetic barrier for the reaction. This barrier would prevent the reaction of V^+ to proceed at room temperature regardless of the efficiency of the spin-forbidden crossing. These results are in agreement with the lack of reaction observed by Koyanagi,[7] results reported here (Table 3), and the absence of reaction in the forward and reverse directions in eq 5 for M = V.[42]

The schematic PES for Ti^+ (Figure 2) is quantitatively different from that of V^+ (Figure 1) showing an increased exothermicity, in agreement with previous theoretical results,[10] and a transition state for the reverse reaction (doublet) located slightly below the reactants energy level, indicating that this reaction might not experience a significant kinetic barrier and that the reaction rate might be dictated instead by the efficiency

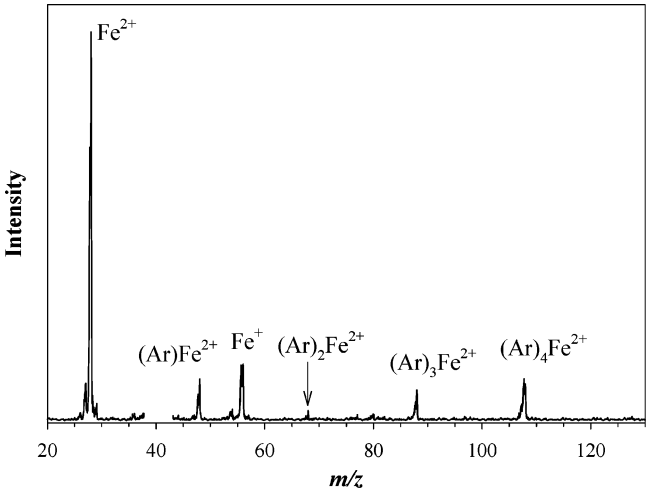

Figure 3. Peak assignment for the spectrum obtained during sputtering Fe with source conditions optimized for the synthesis of Fe^{2+}. Argon flow is approximately 1.6% of the total gas flow.

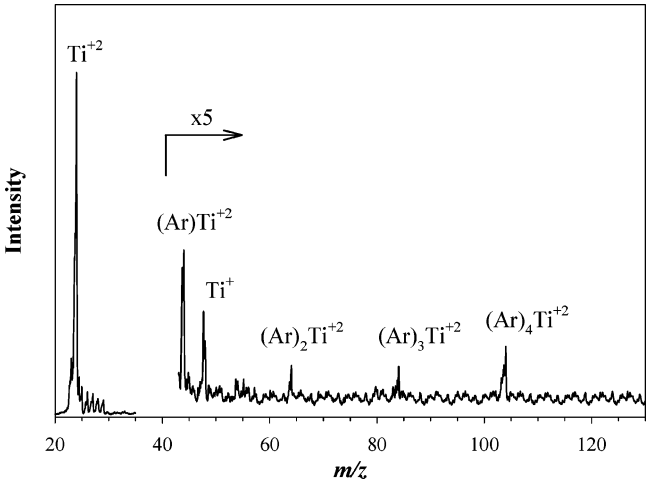

Figure 4. Peak assignment for the spectrum obtained during sputtering Ti with source conditions optimized for the synthesis of Ti^{2+}. Argon flow is approximately 1.7% of the total gas flow.

of the quartet−doublet spin-forbidden surface crossing. The 0.19 value for the efficiency of this reaction (Table 3) suggests that this crossing is relatively efficient.

Formation of Metal Dications. While working on the reactions of Ti^+, V^+, Fe^+, Co^+, Ni^+, Cu^+, and Zn^+ discussed above, we serendipitously discovered a method to generate the dications of V, Ti, and Fe. Furthermore, we were able to detect and identify several other important peaks in the spectra, which was assigned to metal dication−argon cluster species. Generation and detection of the dications of Ti, V, and Fe were accomplished utilizing the same experimental setup used for the generation of the monocations. We found that reduction of the argon sputter gas established conditions leading to the generation and detection of Ti, V, and Fe dications. Optimizing argon flow for each metal dication we investigated was accomplished by monitoring the depletion of the monocation signal in the spectrum and the subsequent appearance of the dication signal in the spectrum while argon flow was adjusted. In this section we show evidence for the synthesis of the dications, discuss possible mechanisms responsible for their generation, and try to elucidate why only the Ti, V, and Fe dications were detected.

Typical spectra with source conditions optimized for the synthesis of Fe^{2+} and Ti^{2+} are shown in Figures 3 and 4, respectively. Whenever possible, peak assignments are made based not only on the peaks' *m*/*z* values but also on the metal isotope distribution, which provides a fingerprint of peaks with separations that are halved in doubly charged species. This feature is clearly seen in Figure 3 for the ^{54}Fe isotope.

The process of sputtering is accomplished by the acceleration of ionized gas atoms, argon for our system, toward a sputter target where collision of the ionized gas with the target surface results in a transfer of kinetic energy. Ionization of the sputtering gas occurs by subjecting the gas to a strong electric potential, greater than 1 kV in our experimental setup, which results in the formation of positive gas ions and electrons. The ionized argon atoms are accelerated toward the target surface, which serves as the cathode, because of the strong negative bias applied. If the amount of kinetic energy transfer during the ion bombardment is of sufficient magnitude, it will result in the ejection of a portion of the cathode surface material and secondary electrons. The ejected cathode material moves from the near surface region, called the cathode dark space, to the glow discharge region where ionization occurs. The observed glow discharge is a result of radiative decay of excited ions and neutral species. Therefore the sputtering and ionization events are separated in space and time.[43]

The sputter process will cause the formation of l metal atoms as well as metal atom clusters. From Figures 3 and 4, it can clearly be seen that we were unable to detect the formation of metal cluster cations [M_n^{x+}; M = Ti, Fe; $n = 2, 3, 4, ...$; $x = 1, 2$], a usual characteristic observed for the metal anions.[44] The failure to observe these cluster ions in our experiments at all possible different source conditions suggests a very efficient ionization process. The highly efficient ionization of the metal clusters would lead to multiple ionization events for each metal cluster by both helium ions and argon ions after being sputtered, which would weaken the metal−metal bonds of the clusters while increasing the formal positive charge of the clusters until a point when columbic repulsive forces exceed the dissociation energy resulting in columbic explosion events leading ultimately to atomic cations as final products.

Ionization in the glow discharge region is accomplished by several mechanisms, including Penning ionization, charge-transfer reactions involving helium and argon ions, and electron impact ionization from fast secondary electrons.[45] While formation of both the monocations and dications is readily accomplished in our system for some metals, we observed that the reduction of argon flowing into our system brought about conditions that allowed for the dications to become the most abundant ion.

We will first examine the case of forming the monocations and then move on to the dications. Formation of the monocations by charge transfer occurs when a metal atom or cluster encounters an ionized argon or helium ion (eqs 6 and 7)

$$Ar^+ + M^0 \rightarrow Ar^0 + M^+ \quad (6)$$

$$He^+ + M^0 \rightarrow M^+ + He^0 \quad (7)$$

$$Ar^* + M^0 \rightarrow Ar^0 + M^+ + e^- \quad (8)$$

$$He^* + M^0 \rightarrow He^0 + M^+ + e^- \quad (9)$$

The charge-transfer reaction is exothermic with both argon and helium for all the metal atoms considered here and thus should be quite efficient (see Table 4). Penning ionization occurs if the metal encounters an excited form of argon or helium (eqs 8 and 9). Ionization may also occur as a result of electron impact

TABLE 4: IPs for Selected Metals and the Ionizing Gases

element	first IP[a]	second IP[a]
Ti	6.83	13.58
V	6.75	14.62
Fe	7.90	16.19
Co	7.88	17.08
Ni	7.64	18.17
Cu	7.73	20.29
Zn	9.39	17.96
He	24.59	54.42
Ar	15.76	27.63

[a] In eV, from ref 27.

provided that the electrons in question possess sufficient energy. Electrons involved in this form of ionization may originate from the cathode surface during sputtering or as a byproduct of ionization events in the glow discharge region.[45]

We propose that the formation of the transition metal dications in our He/Ar mixture DC discharge ion source involves similar ionization mechanisms to those for generation of the monocations and that the generation of both monocations and dications is intimately related with the predominant species being dependent on the argon concentration. Although titanium and vanadium atoms can be ionized to their dications by both Ar^+ or He^+ since the reactions are exothermic (particularly for the latter), the dications of Fe, Co, Ni, Cu, and Zn can only be formed from He^+ (eq 10). (See also Table 4.) Alternatively, ionization by eq 11 is probably less likely due to the columbic repulsive forces operating over long distances decreasing the probability of collision that can lead to such charge-transfer reaction. Penning ionization would be able to ionize both the metal atom and the monocation to the dication form because the metastable helium would not experience the columbic repulsive force that arises between two cations

$$He^+ + M^0 \rightarrow M^{2+} + He^0 + e^- \quad (10)$$

$$He^+ + M^+ \rightarrow He^0 + M^{2+} \quad (11)$$

$$M^{2+} + Ar^0 \rightarrow M^+ + Ar^+ \quad (12)$$

$$He^+ + Ar^0 \rightarrow He^0 + Ar^+ \quad (13)$$

At higher argon flows (about 4−5%) He^+ would react quickly with Ar (eq 13) and the resulting Ar^+ would singly ionize Fe, Co, Ni, Cu, and Zn atoms (or clusters). As discussed above, Ar^+ could also ionize Ti and V atoms to both the cation and dication; however, the cation would predominate as the reaction is substantially more exothermic. This is consistent with our experimental results showing small peaks only for V^{2+} and Ti^{2+} under these source conditions.

At lower argon flows (about 0.5−1.8%) He^+ could live long enough to collide with metal atoms and clusters and doubly ionize them, forming the dications for all metals considered here; however, Fe, Co, Ni, Cu, and Zn would react with argon downstream from the sputter source to form the monocation (eq 12). In other words, even though the dications might be forming for these metals, they would not live long enough after leaving the ion source. On the other hand, eq 12 for M═V, Ti is endothermic and would not occur, in agreement with experimental results showing that the dication is the predominant species for these metals under these source conditions (Table 4). Therefore, the formation of the metal dications requires a trade off between the amount of argon needed to sputter the target and its tendency to quench the dication product at higher argon concentrations. As in the case with Co, Ni, Cu, and Zn, the second ionization potential (IP) of Fe is greater than the first IP of argon (Table 4), which would seem to preclude the observation of Fe^{2+}; however, eq 12 for M═Fe is only slightly exothermic (0.43 eV) and might not be very efficient, as revealed by the prominent peak of Fe^{2+} observed under these source conditions (Figure 3). The formation of $Fe^{2+}(Ar)_n$ clusters seems favored instead.

TABLE 5: Calculated Relative ΔG Values[a] for the Formation of Argon Complexes with Ti^{2+} and Fe^{2+}

species	relative ΔG	species	relative ΔG
$Ti^{2+} + Ar$	0	$Fe^{2+} + Ar$	0
$Ti^{2+}(Ar)_1$	−14.09	$Fe^{2+}(Ar)_1$	−22.67
$Ti^{2+}(Ar)_2$	−22.96	$Fe^{2+}(Ar)_2$	−39.39
$Ti^{2+}(Ar)_3$	−32.07	$Fe^{2+}(Ar)_3$	−48.33
$Ti^{2+}(Ar)_4$	−41.39	$Fe^{2+}(Ar)_4$	−54.78
$Ti^{2+}(Ar)_5$	−38.00	$Fe^{2+}(Ar)_5$	−49.59

[a] In units of kcal/mol and calculated at the B3LYP/6-311G(d) level and 298.16 K as implemented in Gaussian 98 (ref 16).

We observe indeed peaks corresponding to metal argon clusters of the form $[M(Ar)_n]^{2+}$, M = Ti, V, and Fe, $n = 1-4$, see Figures 3 and 4. The formation of argon clusters was not observed for the monocations, even though a much higher argon flow was required in these cases. The formation of the dication−argon clusters arises from electrostatic interactions between the positive metal dication and the polarizable argon atom, which is enhanced in this case by the double charge in the metal center. Formation of the metal dication argon clusters is thought to occur in a stepwise fashion in our system with the dication forming first followed by the addition of the subsequent argon atoms.

Theoretical results on the binding energies of the $M^{2+}(Ar)_n$ clusters for M = Ti, Fe ($n = 1-5$) are listed in Table 5, showing that the formation of theses clusters is very exoergic. The sequential addition of individual argon atoms is favorable until a maximum of four is reached; further addition of an argon atom to the $M^{2+}(Ar)_4$ clusters is endoergic and therefore would not be expected to occur. These results are in excellent agreement with spectra of Fe and Ti shown in Figures 3 and 4, displaying the absence of peaks at m/z 128 for $[Fe(Ar)_5]^{2+}$ (Figure 3) and m/z 124 corresponding to $[Ti(Ar)_5]^{2+}$ (Figure 4).

The results included in Table 5 also show that the formation of the $Fe^{2+}(Ar)_n$ clusters are substantially more exoergic than those involving Ti^{2+}, which is due to the smaller ionic radius in Fe^{2+} since the bonding in these clusters is essentially electrostatic in nature. These results are also in excellent agreement with experimental results shown in Figures 3 and 4, showing more intense cluster peaks for Fe than for Ti at essentially the same argon concentration.

As mentioned above, the reaction shown in eq 12 for M═Fe is slightly exothermic (0.43 eV); however, the formation of the $Fe^{2+}(Ar)_1$ is even more favorable (22.67 kcal/mol = 0.98 eV) and therefore the cluster is stable with respect to the dissociation into Fe^+ and Ar^+. Doubly charged cations of Co, Ni, Cu, and Zn would form even more stable clusters with argon due to the smaller ionic radii; however, the second IP in these metals increases faster producing metastable clusters (i.e., the dissociation into M^+ and Ar^+ is exothermic). This issue has been discussed in detail elsewhere.[46−49] The absence of dication−argon clusters for Co, Ni, Cu, and Zn in our spectra is consistent with the sequential formation of these clusters in our experimental setup. Formation of these metastable clusters seems to be observed only in ion source conditions in which the neutral clusters are formed first and then doubly ionized (charge stripping).[50,51]

Conclusions

The reactions of selected transition metal cations with carbon monoxide and carbon dioxide have been studied. Metal cations were synthesized by using a sputter ion source. We also observed the metal dications could selectively be made by adjusting the ion source conditions.

Metal cations−CO complexes were the sole reaction product observed in the reactions of monocations with CO. Reaction rates are slow in general and in some cases are below our detection limit. The fastest reactions in this group are for Cu^+ and Ni^+ where a second addition of CO is also observed. Reactivity seems to follow the M−CO bond dissociation energy.

Reactions of metal cations with CO_2 are slightly larger, and we report rates that are in reasonable agreement with lower limit values reported recently. While most of the metal cations form complexes with CO_2, Ti^+ reacts with CO_2 yielding TiO^+. This C−O activation process occurs very efficiently despite a required spin-forbidden curve crossing.

We also report the first experiments in producing multiply charged metal cations using a sputter ion source. Metal dications can be easily synthesized for metals with a second IP comparable to or lower than the IP for argon, which is required for the sputtering process. Despite the low argon concentration conditions, the doubly charged cations readily form argon clusters, $M^{2+}(Ar)_n$ [M = Ti, V, Fe (n = 1−4)]. Experimental evidence suggests that these clusters are formed in a stepwise mechanism.

In principle, changing the sputter gas from argon to Ne (IP = 21.56 eV) would increase the number of metals in which double charged cations can be made, hopefully without compromising sputtering efficiency. Experiments are being conducted in our lab to test this hypothesis.

Acknowledgment. We gratefully acknowledge the support for this work from the University of Idaho and the NASA Idaho Space Grant Consortium. J.D.F thanks the NSF R.E.U. program for financial support.

References and Notes

(1) Ferguson, E. E.; Fehsenfeld, F. C.; Schmeltekopf, A. L. *Adv. At. Mol. Phys.* **1969**, *5*, 1.
(2) Pickett, C. J.; Vincent, K. A.; Ibrahim, S. K.; Gormal, C. A.; Smith, B. E.; Fairhurst, S. A.; Best, S. P. *Chem.−Eur. J.* **2004**, *10*, 4770.
(3) Tielens, A. G. G. M.; Wooden, D. H.; Allamandola, L. J.; Bregman, J.; Witteborn, F. C. *Astrophys. J.* **1996**, *461*, 210.
(4) Koyanagi, G. K.; Lavrov, V. V.; Baranov, V.; Bandura, D.; Tanner, S.; McLaren, J. W.; Bohme, D. K. *Int. J. Mass Spectrom.* **2000**, *194*, L1.
(5) Jarvis, M. J. Y.; Pisterzi, L. F.; Blagojevic, V.; Koyanagi, G. K.; Bohme, D. K. *Int. J. Mass Spectrom.* **2003**, *227*, 161.
(6) Baranov, V.; Javahery, G.; Hopkinson, A. C.; Bohme, D. K. *J. Am. Chem. Soc.* **1995**, *117*, 12801.
(7) Koyanagi, G. K.; Bohme, D. K. *J. Phys. Chem. A* **2006**, *110*, 1232.
(8) Caraiman, D.; Koyanagi, G. K.; Scott, L. T.; Preda, D. V.; Bohme, D. K. *J. Am. Chem. Soc.* **2001**, *123*, 8573.
(9) Sievers, M. R.; Armentrout, P. B. *J. Chem. Phys.* **1995**, *102*, 754.
(10) Sodupe, M.; Branchadell, V.; Rosi, M.; Bauschlicher, C. W., Jr. *J. Phys. Chem. A* **1997**, *101*, 7854.
(11) Bierbaum, V. M.; DePuy, C. H.; Shapiro, R. H.; Stewart, J. H. *J. Am. Chem. Soc.* **1976**, *98*, 4229.
(12) Davico, G. E. *J. Phys. Chem. A* **2005**, *109*, 3433.
(13) Ho, J.; Ervin, K. M.; Lineberger, W. C. *J. Chem. Phys.* **1990**, *93*, 6987.
(14) Ho, J. Negative Ion Laser Photoelectron Spectroscopy of Mass Selected Small Metal Clusters. Ph.D. Thesis, University of Colorado, 1991.
(15) Steinfeld, J. I.; Francisco, J. S.; Hase, W. L. *Chemical Kinetics and Dynamics, Second Edition*; Prentice Hall: Upper Saddle River, NJ, 1999.
(16) Frisch, M. J.; Trucks, G. W.; Schlegel, H. B.; Scuseria, G. E.; Robb, M. A.; Cheeseman, J. R.; Zakrzewski, V. G.; Montgomery, J. A.; Stratmann, R. E.; Burant, J. C.; Dapprich, S.; Millam, J. M.; Daniels, A. D.; Kudin, K. N.; Strain, M. C.; Farkas, O.; Tomasi, J.; Barone, V.; Cossi, M.; Cammi, R.; Mennucci, B.; Pomelli, C.; Adamo, C.; Clifford, S.; Ochterski, J.; Petersson, G. A.; Ayala, P. Y.; Cui, Q.; Morokuma, K.; Malick, D. K.; Rabuck, A. D.; Raghavachari, K.; Foresman, J. V.; Cioslowski, J.; Ortiz, J. V.; Baboul, A. G.; Stefanov, B. B.; Liu, G.; Liashenko, A.; Piskorz, P.; Komaromi, I.; Gomperts, R.; Martin, R. L.; Fox, D. J.; Keith, T.; Al-Laham, M. A.; Peng, C. Y.; Nanayakkara, A.; Gonzales, C.; Challacombe, M.; Gill, P. M. W.; Johnson, B.; Chen, W.; Wong, M. W.; Andres, J. L.; Head-Gordon, M.; Replogle, E. S.; Pople, J. A. *Gaussian 98*, revision A.9; Gaussian, Inc.: Pittsburgh, PA, 1998.
(17) Becke, A. D. *J. Chem. Phys.* **1992**, *96*, 2155.
(18) Becke, A. D. *J. Chem. Phys.* **1993**, *98*, 5648.
(19) Lee, C.; Yang, W.; Parr, R. G. *Phys. Rev. B* **1988**, *37*, 785.
(20) Dunning, T. H., Jr. *J. Chem. Phys.* **1989**, *90*, 1007.
(21) Woon, D. E.; Dunning, T. H., Jr. *J. Chem. Phys.* **1993**, *98*, 1358.
(22) Clemmer, D. E.; Elkind, J. L.; Aristov, N.; Armentrout, P. B. *J. Chem. Phys.* **1991**, *95*, 3387.
(23) Mallard, W. G.; Linstrom, P. J. NIST Chemistry WebBook, NIST Standard Reference Database Number 69. (http://webbook.nist.gov); National Institute of Standards and Technology: Gaithersburg MD, 1998.
(24) Su, T.; Chesnavich, W. J. *J. Chem. Phys.* **1982**, *76*, 5183.
(25) Jarvis, M. J. Y.; Blagojevic, V.; Koyanagi, G. K.; Bohme, D. K. *Eur. J. Mass Spectrom.* **2004**, *10*, 949.
(26) Lavrov, V. V.; Blagojevic, V.; Koyanagi, G. K.; Orlova, G.; Bohme, D. K. *J. Phys. Chem. A* **2004**, *108*, 5610.
(27) Sansonetti, J. E.; Martin, W. C.; Young, S. L. Handbook of Basic Atomic Spectroscopic Data (version 1.1.2) (http://physics.nist.gov/Handbook); National Institute of Standards and Technology, Gaithersburg, MD, 2005.
(28) Khan, F. A.; Steele, D. L.; Armentrout, P. B. *J. Phys. Chem.* **1995**, *99*, 7819.
(29) Goebel, S.; Haynes, C. L.; Khan, F. A.; Armentrout, P. B. *J. Am. Chem. Soc.* **1995**, *117*, 6994.
(30) Schultz, R. H.; Crellin, K. C.; Armentrout, P. B. *J. Am. Chem. Soc.* **1991**, *113*, 8590.
(31) Sievers, M. R.; Armentrout, P. B. *J. Phys. Chem.* **1995**, *99*, 8135.
(32) Meyer, F.; Chen, Y.-M.; Armentrout, P. B. *J. Am. Chem. Soc.* **1995**, *117*, 4071.
(33) Meyer, F.; Armentrout, P. B. *Mol. Phys.* **1996**, *88*, 187.
(34) Barnes, L. A.; Rosi, M.; Bauschlicher, C. W., Jr. *J. Chem. Phys.* **1990**, *93*, 609.
(35) Gutsev, G. L.; Andrews, L.; Bauschlicher, C. W. *Chem. Phys.* **2003**, *290*, 47.
(36) Glaesemann, K. R.; Gordon, M. S.; Nakano, H. *Phys. Chem. Chem. Phys.* **1999**, *1*, 967.
(37) Armentrout, P. B.; Koizumi, H.; MacKenna, M. *J. Phys. Chem. A* **2005**, *109*, 11365.
(38) Dieterle, M.; Harvey, J. N.; Heinemann, C.; Schwarz, J.; Schroeder, D.; Schwarz, H. *Chem. Phys. Lett.* **1997**, *277*, 399.
(39) Schwarz, J.; Schwarz, H. *Organometallics* **1994**, *13*, 1518.
(40) Asher, R. L.; Bellert, D.; Buthelezi, T.; Weerasekera, G.; Brucat, P. J. *Chem. Phys. Lett.* **1994**, *228*, 390.
(41) Herman, J.; Davico, G. E. Manuscript in preparation.
(42) Kappes, M. M.; Staley, R. H. *J. Am. Chem. Soc.* **1981**, *103*, 1286.
(43) Betti, M.; Aldave de las Heras, L. *Spectrosc. Eur.* **2003**, *15*, 15.
(44) Leopold, D. G.; Ho, J.; Lineberger, W. C. *J. Chem. Phys.* **1987**, *86*, 1715.
(45) Bogaerts, A.; Gijbels, R. *Spectrochim. Acta B* **1998**, *53B*, 1.
(46) Schroeder, D.; Schwarz, H. *J. Phys. Chem. A* **1999**, *103*, 7385.
(47) Stace, A. J. *J. Phys. Chem. A* **2002**, *106*, 7993.
(48) Tonkyn, R.; Weisshaar, J. C. *J. Am. Chem. Soc.* **1986**, *108*, 7128.
(49) Stace, A. J. *Adv. Metal Semiconduct. Clust.* **2001**, *5*, 121.
(50) Walker, N. R.; Grieves, G. A.; Jaeger, J. B.; Walters, R. S.; Duncan, M. A. *Int. J. Mass Spectrom.* **2003**, *228*, 285.
(51) Walker, N. R.; Wright, R. R.; Barran, P. E.; Cox, H.; Stace, A. J. *J. Chem. Phys.* **2001**, *114*, 5562.